JOURNAL OF VIROLOGY, Oct. 1994, p. 6523–6534
0022-538X/94/$04.00+0

Vol. 68, No. 10

# Coronavirus M Proteins Accumulate in the Golgi Complex beyond the Site of Virion Budding

JUDITH KLUMPERMAN,[1]* JACOMINE KRIJNSE LOCKER,[2] ADAM MEIJER,[2] MARIAN C. HORZINEK,[2] HANS J. GEUZE,[1] AND PETER J. M. ROTTIER[2]

*Department of Cell Biology, Center for Electronmicroscopy, Utrecht University, 3584 CX Utrecht,[1] and Department of Infectious Diseases and Immunology, Virology Division, Utrecht University, 3584 CL Utrecht,[2] The Netherlands*

Received 1 February 1994/Accepted 30 June 1994

**The prevailing hypothesis is that the intracellular site of budding of coronaviruses is determined by the localization of its membrane protein M (previously called E1). We tested this by analyzing the site of budding of four different coronaviruses in relation to the intracellular localization of their M proteins. Mouse hepatitis virus (MHV) and infectious bronchitis virus (IBV) grown in Sac(−) cells, and feline infectious peritonitis virus (FIPV) and transmissible gastroenteritis virus (TGEV) grown in CrFK cells, all budded exclusively into smooth-walled, tubulovesicular membranes located intermediately between the rough endoplasmic reticulum and Golgi complex, identical to the so-called budding compartment previously identified for MHV. Indirect immunofluorescence staining of the infected cells showed that all four M proteins accumulated in a perinuclear region. Immunogold microscopy localized MHV M and IBV M in the budding compartment; in addition, a dense labeling in the Golgi complex occurred, MHV M predominantly in *trans*-Golgi cisternae and *trans*-Golgi reticulum and IBV M mainly in the *cis* and medial Golgi cisternae. The corresponding M proteins of the four viruses, when independently expressed in a recombinant vaccinia virus system, also accumulated in the perinuclear area. Quantitative pulse-chase analysis of metabolically labeled cells showed that in each case the majority of the M glycoproteins carried oligosaccharide side chains with Golgi-specific modifications within 4 h after synthesis. Immunoelectron microscopy localized recombinant MHV M and IBV M to the same membranes as the respective proteins in coronavirus-infected cells, with the same *cis-trans* distribution over the Golgi complex. Our results demonstrate that some of the M proteins of the four viruses are transported beyond the budding compartment and are differentially retained by intrinsic retention signals; in addition to M, other viral and/or cellular factors are probably required to determine the site of budding.**

Coronaviruses acquire their lipoprotein envelope by budding at intracellular membranes (for reviews, see references 10 and 39). Within this envelope are at least two viral glycoproteins, the membrane protein M (previously referred to as E1) and the spike protein S (formerly E2). The M protein has been found to play a key role in determining the site of budding, mainly on the basis of two types of experiments (for reviews, see references 34, 49, and 52). First, virus budding and release are not affected by tunicamycin, a drug which inhibits N-linked glycosylation (13, 41, 51). The virus particles released under these conditions contain M but lack S, suggesting that M is the only envelope glycoprotein required for budding. Second, M is the only viral protein whose intracellular distribution correlates with the sites of budding (57). In the murine cell line Sac(−), early MHV budding was found to occur at smooth tubulovesicular membranes that were often located in close proximity to the Golgi complex and the rough endoplasmic reticulum (RER). These membranes were consequently termed the budding compartment (57). At later times, the RER became the major site of budding. By means of immunofluorescence and immunoperoxidase electron microscopy, the M protein of mouse hepatitis virus (MHV) was first found in the budding compartment and only later in the RER, coinciding with the onset of budding in these two compartments. It was concluded that accumulation of M determines the time and site of budding, a view which is now widely accepted (see reviews by Griffiths and Rottier [10], Niemann et al. [34], Petterson [39], Spaan et al. [49], and Sturman and Holmes [52]). The identification of the budding compartment and the RER as exclusive budding sites is in agreement with early electron microscopic observations on the budding of MHV and infectious bronchitis virus (IBV) (2, 5, 7). The budding sites of other coronaviruses have not been characterized in detail.

Over the last years, however, data that cast doubt on the role of the M protein as the sole determinant of the site of budding have been reported. First, the intracellular retention of MHV M may not be representative of all coronavirus M proteins. Conflicting data exist on the localization of the M protein of transmissible gastroenteritis virus (TGEV) of swine. Laviada et al. (25) and To et al. (55) reported that TGEV M was present at the plasma membrane of TGEV-infected cells, whereas according to Pulford and Britton (40), TGEV M remained intracellularly. Also, the M protein of feline infectious peritonitis virus (FIPV) has been found to reach the plasma membrane of infected cells (16). The M proteins of other coronaviruses have not been localized.

Second, when MHV M (35, 42) and IBV M (30) were independently expressed from cloned cDNA, the recombinant proteins accumulated intracellularly, indicating that their retention is caused by an intrinsic signal, independent on the presence of other viral proteins. However, biochemical analysis of the oligosaccharide chains of recombinant MHV M revealed that the protein acquires modifications specific for the *trans*-Golgi cisternae/*trans*-Golgi reticulum (TGR); this finding is in agreement with immunogold labeling data, which localized M throughout the Golgi complex and in the TGR (22).

* Corresponding author. Present address: Graduate School Neurosciences Amsterdam, Vrije University, Faculty of Biology, Boelelaan 1087, 1081 HV Amsterdam, The Netherlands. Phone: 31205482918. Fax: 31206429202.

Accordingly, the N-linked sugar chains of a small portion of recombinant IBV M protein acquired endoglycosidase H (endo H) resistance (30, 54), indicating that at least a portion of the protein reaches the medial Golgi (20). By means of immunoelectron microscopy, IBV M was indeed localized in the Golgi complex, predominantly at the *cis* side. In contrast, the N-linked oligosaccharide chains of TGEV M and FIPV M did not acquire endo H resistance when expressed independently (40, 59). Their exact intracellular localization has not been determined. All coronavirus M proteins are triple-spanning membrane glycoproteins with well-conserved secondary structures, which bear either N-linked or O-linked oligosaccharide chains (for reviews, see references 34 and 49). It is unknown how these proteins are retained in intracellular membranes; both transmembrane and nontransmembrane domains of the protein are involved (1, 28–30).

Collectively, these data led us to reconsider the presumed role of M protein in the coronavirus budding process. To extend the data from MHV to other coronaviruses, we included IBV, FIPV, and TGEV and established the site of budding and the localization of the respective M proteins. We chose to do this early in infection, i.e., before the onset of cytopathology. Our studies show that all four coronaviruses bud into similar pre-Golgi membranes, but that the respective M proteins, regardless whether other viral proteins are present, accumulate at intracellular membranes beyond the natural site of budding. We conclude that accumulation of M protein alone is not sufficient to localize the budding.

## MATERIALS AND METHODS

**Viruses and cells.** The following coronaviruses were used: MHV strain A59, IBV strain M41, FIPV strain 79-1146 (31), and TGEV strain Purdue. MHV was propagated in the murine cell line Sac(−), concentrated, and titrated as described before (50). IBV was adapted to Sac(−) cells by two serial passages at a low multiplicity of infection. Concentrated stocks were prepared as for MHV, and the virus was quantitated by endpoint titration in the same cells. Infection of up to 50% of the cells could be achieved with these stocks, allowing the comparative study of IBV and MHV in the same cell type. Since FIPV and TGEV do not grow in Sac(−) cells, these viruses were propagated in and titrated by limiting dilution on *Felis catus* whole fetus (fcwf-D) cells and pig kidney (PD5) cells, respectively. In addition, infection experiments with these viruses were done in Crandell feline kidney (CrFK) cells and Norden Laboratories feline kidney (NLFK) cells. All cells were grown in Dulbecco's minimal essential medium (DMEM) containing penicillin, streptomycin, and 5% heat-inactivated fetal calf serum (FCS) and plated 1 day before each experiment.

The construction of the recombinant vaccinia viruses expressing MHV-M (referred to here as vvMHV-M) and IBV-M (vvIBV-M) have been described elsewhere (23, 29). vvFIPV-M had been constructed as described by Vennema et al. (59). The preparation of vvTGEV-M is described below. For the expression of recombinant vaccinia viruses, we used the human hepatoma cell line HepG2, which was cultured in DMEM supplemented with penicillin, streptomycin, and 10% FCS. HepG2 cells were plated 5 days before each experiment.

**Construction of recombinant vaccinia virus expressing TGEV-M.** Recombinant DNA techniques were performed essentially as described by Sambrook et al. (43). The TGEV cDNA clone A6 prepared by Jacobs et al. (15) was used as a source of the M gene. A subclone of A6 was first made by *Hin*dIII digestion and self-ligation of this pUC9-based plasmid, thereby removing most part of the S gene. The M gene was excised from the plasmid by cutting with *Pst*I, *Hgi*AI, and *Bgl*I, the relevant fragment was purified, and the DNA was blunted with mung bean exonuclease and ligated into the *Sma*I-digested vaccinia virus transfer vector pSC11 (3). Clone L10, which has the M gene in the correct orientation for expression from the early vaccinia virus promoter P7.5, was selected, and a recombinant vaccinia virus expressing the M gene was prepared as described by Machamer and Rose (30).

**Antibodies.** For immunolabeling of MHV M, we used a rabbit antiserum raised against a synthetic peptide corresponding to the COOH-terminal 18 amino acids of MHV M (23). IBV M was detected by using rabbit antiserum 4735, raised against a synthetic peptide corresponding to the IBV M COOH-terminal 22 amino acids (30). FIPV M and TGEV M were detected with the mouse monoclonal antibodies Cor 21 and Cor 16, respectively. The specificity of the antibodies was confirmed by the absence of label in noninfected cells (not shown). Cor 21 and Cor 16 could be used for immunofluorescence only, since the fixative used for immunoelectron microscopy (see below) abolished the labeling; fixation with 2% formaldehyde preserved the labeling but resulted in poor overall morphology. To immunolocalize the cation-independent mannose 6-phosphate receptor (CI-MPR), galactosyltransferase, and clathrin we used affinity-purified rabbit antibodies previously described (8, 12). The antibody against p53 has been described elsewhere (45).

**Immunofluorescence and electron microscopy.** For immunofluorescence, cells were fixed at 4, 6, and 8 h postinfection (p.i.) in 3% paraformaldehyde in phosphate-buffered saline (PBS; pH 7.4) for 30 min at room temperature. Subsequent permeabilization and staining were performed as described previously (6).

For conventional electron microscopy, cells were fixed in 2% glutaraldehyde–0.25 mM $CaCl_2$–0.25 mM $MgCl_2$ in 80 mM sodium cacodylate buffer (pH 7.4) for 1 h at room temperature. After postfixation for 30 min in 1% $OsO_4$ in 0.1 M sodium cacodylate (pH 7.4), cells were dehydrated, embedded in Epon, and contrasted as described previously (18).

Cells were fixed for cryoelectron microscopy by adding a mixture of 0.2% glutaraldehyde and 2% acrolein in 0.1 M phosphate buffer (pH 7.4) to an equal volume of medium. After 2 h of incubation at room temperature, the fixative was removed by three rinses with PBS. Cells were then scraped with a rubber policeman and washed three times with 0.15% glycine in PBS. After resuspension in 10% gelatin in PBS and preparation of 1-$mm^3$ blocks at 4°C, cells were impregnated with 2.3 M sucrose and frozen in liquid nitrogen. Cryosections were prepared, immunolabeled, and double immunolabeled as described previously (47, 48).

The density of MHV M representing gold particles was determined as follows. Infected cells were selected, and the area of interest was projected at a magnification of ×12,000 onto a television screen connected to a JEOL 1200 EX electron microscope. As an arbitrary unit for measuring membrane length, we counted the number of intersections of the membrane in question with a line raster (width of 1 cm) superimposed on the television screen. The density of the gold particles was expressed as number of gold particles per intersection (60).

**Metabolic labeling and immunoprecipitation.** HepG2 cells were grown to confluency in 5 days in 35-mm-diameter dishes and infected at a high multiplicity of infection with vvMHV-M, vvFIPV-M, or vvTGEV-M. At 4.5 h p.i., the cells were incubated for 30 min in 0.6 ml of methionine-free minimal essential medium (Gibco, Life Technologies Ltd, Paisley,

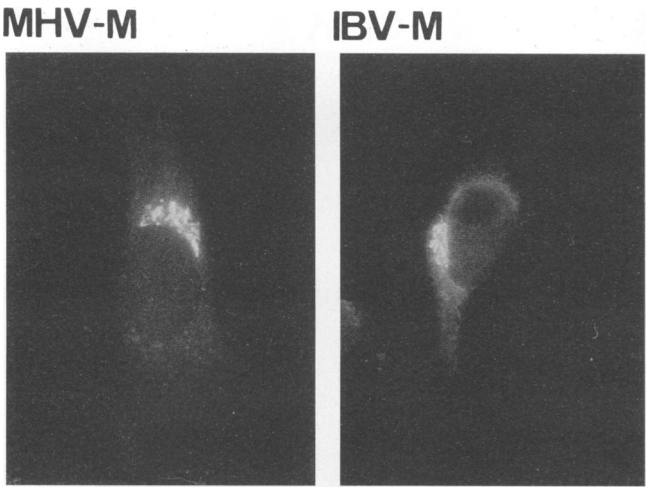


FIG. 1. Immunofluorescence staining for MHV-M and IBV-M in Sac(−) cells at 6 and 8 h p.i., respectively. Both M proteins are retained in the perinuclear area.

Scotland) containing 2% FCS. Then cells were labeled for 1 h with 150 μCi of [$^{35}$S]methionine ([$^{35}$S]Express label; NEN/Dupont, 's Hertogenbosch, The Netherlands) and chased for 3 h with 2 mM methionine in DMEM–10% FCS. Similarly, vvIBV-M-infected cells were preincubated in cysteine-free minimal essential medium, labeled with [$^{35}$S]cysteine (Amersham International, Amersham, England), and chased with 2 mM cysteine. Cells were lysed, and the M proteins were immunoprecipitated as described (23). Neuraminidase (*Arthrobacter ureafaciens*; Boehringer GmbH, Mannheim, Germany) treatment was carried out as described previously (22). Endo H and *N*-glycanase (Boehringer) digestions were done as described by Machamer et al. (29). Quantification of the protein bands on the autoradiograms was carried out as described by Suissa (53).

## RESULTS

**Coronavirus infections.** To determine an early time point at which detectable levels of M proteins had been synthesized and to establish its overall distribution, infected cells were analyzed by immunofluorescence at several time periods after infection. In Sac(−) cells at 6 h after MHV infection and 8 h after IBV infection, the respective M proteins were readily detectable. The label was confined to the cytoplasm, where it occurred as distinct spots in the perinuclear area (Fig. 1). The plasma membrane was devoid of label, and nonpermeabilized cells labeled with an antibody against the N-terminal part of MHV M were not reactive (not shown). Because of their different tropisms, a feline cell line was selected for FIPV and TGEV. To avoid any cell-type-specific bias, we first investigated three different cell lines (fcwf-D, NLFK, and CrFK) and compared the patterns of expression of the respective M proteins by immunofluorescence. In all three cell lines, both FIPV M and TGEV M were distinctly expressed at 6 h p.i. (Fig. 2), showing identical distribution patterns. Label was always concentrated in distinct spots in the perinuclear area. An additional labeling, appearing as a punctate pattern throughout the cytoplasm, was seen only in FIPV-infected NLFK cells. No label could be detected at the plasma membrane. The fluorescence staining was most intense in the CrFK cells, which led us to choose this line for subsequent studies.

**Determination of the initial sites of budding.** On the basis of the immunofluorescence data, we next analyzed the budding sites of the respective viruses and the subcellular distribution of their M proteins at 6 h p.i. (MHV, FIPV, and TGEV infection) and at 8 h p.i. (IBV infection). Figures 3 to 5 show the early sites of budding of the four coronaviruses as they appeared in ultrathin sections of plastic-embedded cells. In agreement with the observations of Tooze et al. (57), we found budding profiles of MHV in Sac(−) cells only in smooth-surfaced membranes, adjacent to the Golgi complex, which these authors had designated the MHV budding compartment (Fig. 3A). Budding profiles of IBV were exclusively observed in the same types of smooth membranes where MHV was found to assemble (Fig. 3B to D). Within the Golgi complex of IBV-infected cells, only assembled virus particles were found (Fig. 3B), always at the rims of the cisternae, consistent with the notion that budding of IBV is a pre-Golgi event. The membranes of the budding compartment form a rather extensive network in the cell (Fig. 3C) (21), often found in close proximity to the RER. However, budding of IBV into the RER was not observed at this time of infection (6 h p.i.) (Fig. 3D). Beyond the Golgi complex, the newly formed IBV particles accumulated within collecting vesicles (Fig. 3B).

Budding of FIPV and TGEV in CrFK cells was studied at 6 h p.i. As illustrated in Fig. 4 and 5, budding was again restricted to smooth-surface membranes in the Golgi area. These membranes were morphologically identical to the budding compartment in Sac(−) cells (Fig. 3). Budding profiles or assembled particles were absent from the RER. In the Golgi complex, only free virus particles were seen (Fig. 4B and insert in Fig. 5). Beyond the Golgi complex, the virus particles were seen in collecting vesicles containing variable numbers of particles (not shown). CrFK cells infected with either virus were morphologically indistinguishable.

We conclude from these data that early in the infection cycle, all four coronaviruses bud exclusively at pre-Golgi membranes, presumably of the budding compartment as originally defined for MHV (57).

**Subcellular localization of M proteins in coronavirus-infected cells.** To establish the intracellular localization of M proteins at the time of progeny virion formation, we prepared Sac(−) cells for immunocytochemistry at 6 and 8 h after MHV and IBV infection, respectively. In cryosections, the budding compartment could be recognized as a network of smooth-surfaced membranes harboring progeny virions and occasionally showing budding profiles (e.g., Fig. 6A). The budding profiles were more difficult to detect than in plastic sections, probably because of the negative staining of membranes in cryosections. The antibodies used in this study were directed against the COOH termini of the respective M proteins. It should be noted that the C terminus of free M protein is on the cytoplasmic side of the intracellular membranes, but that it points toward the virion interior after budding. Immunogold labeling revealed the presence of free MHV M and IBV M in the membranes of the budding compartment (Fig. 6A and C) and in the Golgi complex (Fig. 6B, D, and E). Other membranes, including the RER and the plasma membrane, were devoid of label (not shown).

Within the Golgi complex, MHV M and IBV M showed different distribution patterns. MHV M was found in all cisternae, with occasional label in the TGR (Fig. 6B), whereas IBV M was predominantly found at the *cis* side of the Golgi complex (Fig. 6D and E), as shown by double immunolabeling of IBV M and clathrin. Clathrin is mainly located at the *trans* side of the Golgi complex (9, 36, 37). Morphologically, clathrin-coated vesicles were readily distinguishable from non-

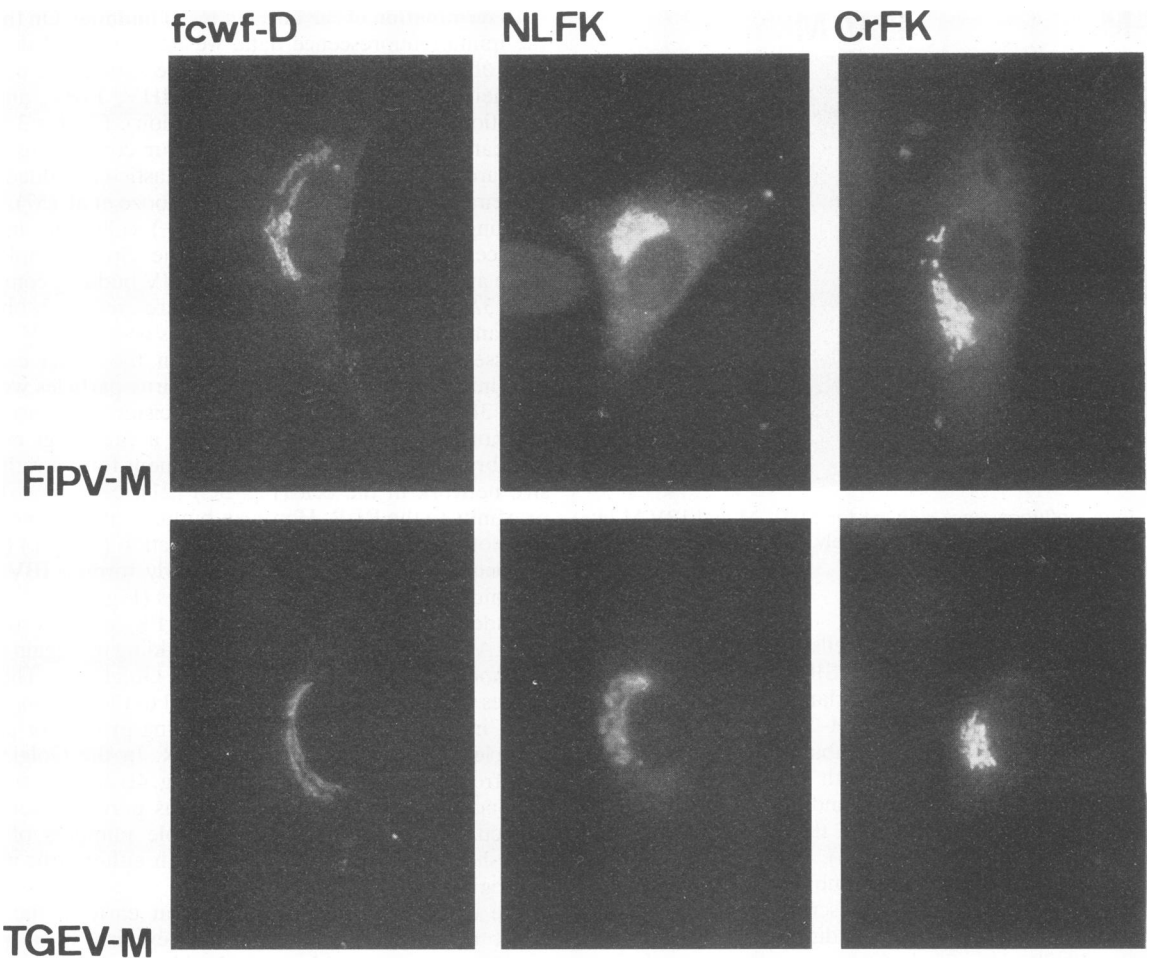


FIG. 2. Immunofluorescence staining of FIPV-M and TGEV-M in fcwf-D, NLFK, and CrFK cells at 6 h p.i. In all three cell lines, both M proteins accumulate in the perinuclear area.

clathrin-coated vesicles, which reside predominantly at the *cis* side and the rims of the Golgi complex (36).

A striking observation was the high density of labeling of the Golgi cisternae compared with the budding compartment (compare Fig. 6A with Fig. 6B and Fig. 6C with Fig. 6D and E). This was confirmed when we counted the number of gold particles for M protein per unit length of membrane and compared both labeling densities. We chose to do this in MHV-infected cells, since the preferential localization of MHV M at the *trans* side of the Golgi stacks allowed a good distinction between membranes of the Golgi complex and the budding compartment. As shown in Table 1, the concentration of MHV M protein in membranes of the Golgi complex within one cell was generally found to be within the same range as or higher than in membranes of the budding compartment. Analysis of these data with the Student *t* test showed that on average, the labeling density of the Golgi membranes was significantly higher than the labeling density of the membranes of the budding compartment ($P = 0.019$, $t = 3.18$).

These data show that while budding occurs exclusively in the budding compartment, large amounts of M proteins reach the Golgi complex.

**Expression of M proteins in HepG2 cells by recombinant vaccinia viruses.** To determine the intracellular localization of M protein in the absence of other coronaviral proteins, we studied the vaccinia virus recombinants vvMHV-M, vvIBV-M, vvFIPV-M, and vvTGEV-M after infection of the human hepatoma cell line HepG2. The use of these cells allowed us to identify compartments of the early biosynthetic pathway not only by morphological criteria but also by immunolabeling of established marker proteins (see below). The expression levels of the recombinant M proteins at various times during infection as well as their overall distribution were analyzed by immunofluorescence. At 6 h p.i., all recombinant M proteins were expressed in most cells, though the expression level per cell varied considerably. Fluorescence for all four M proteins was similar to that in coronavirus-infected cells and was concentrated in spots close to the nucleus (Fig. 7), whereas no label was detected at the plasma membrane.

**Biochemical analysis of independently expressed M protein.** We first determined the transport of the respective recombinant M proteins biochemically, making use of the fact that all M proteins acquire O-linked (MHV M [33]) or N-linked (IBV M [51], TGEV M [24], and FIPV M [59]) oligosaccharides. Infected HepG2 cells were metabolically labeled for 1 h and chased in the absence of radioactivity for 3 h (Fig. 8). Transport of vvMHV-M could be monitored by the appearance of the different O-glycosylated forms (designated $M_0$ to $M_4$), which have been characterized in detail in a previous study (22). During the labeling period, a significant part of the M

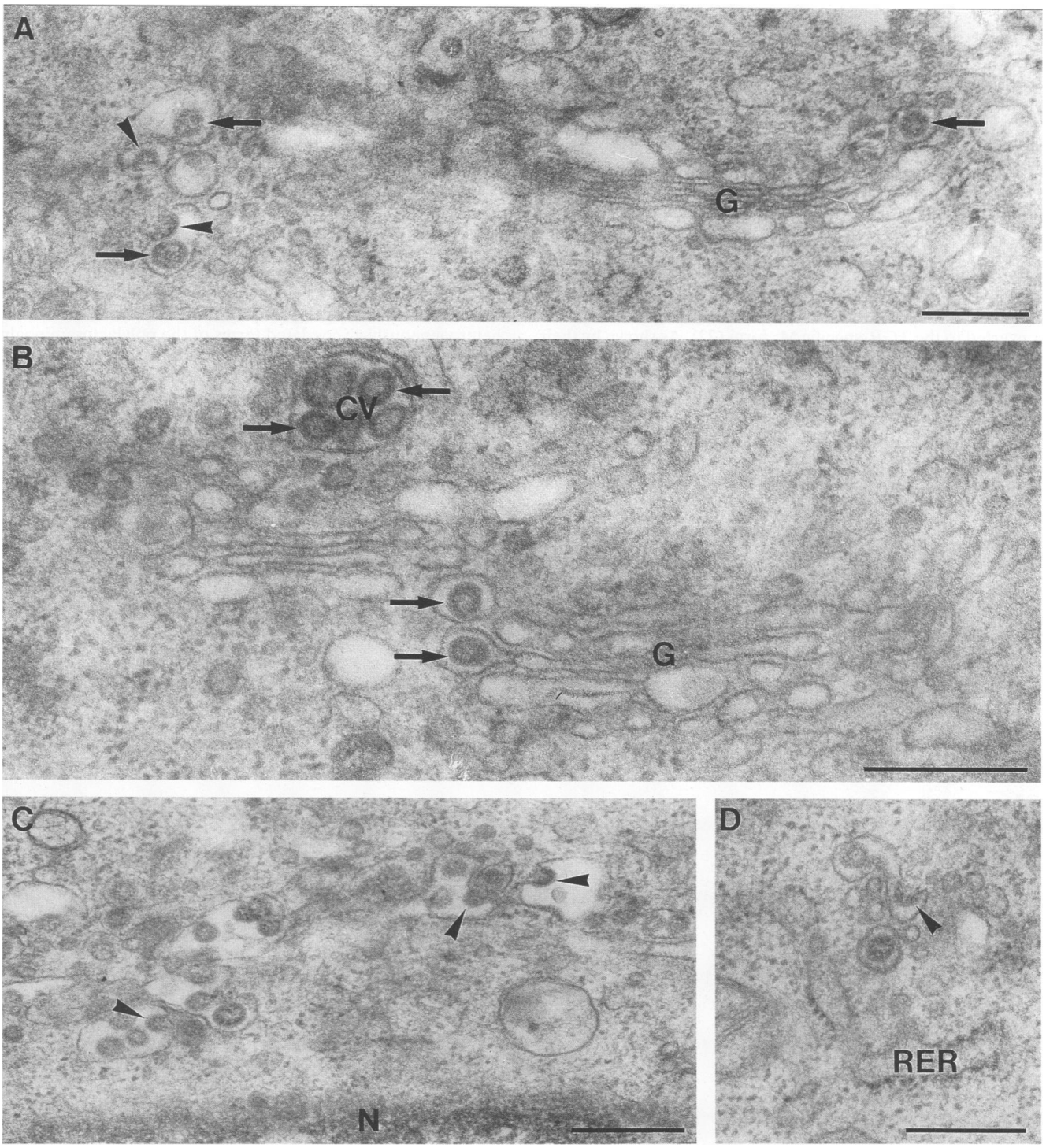


FIG. 3. Budding profiles (arrowheads) and apparently free viruses (arrows) of MHV (A) and IBV (B to D) in coronavirus-infected Sac(−) cells at 6 and 8 h p.i., respectively. (A) MHV budding profiles in smooth-surfaced membranes near the Golgi complex (G). Within the Golgi complex, only apparently free viruses are seen. (B) Golgi complex harboring apparently free IBV particles. Post-Golgi, the viruses accumulate in collecting vesicles (CV). (C) IBV budding profiles in smooth-surfaced membranes near the nucleus (N). (D) IBV budding profiles in smooth-surfaced membranes closely apposed to the RER. Bars, 0.1 μm.

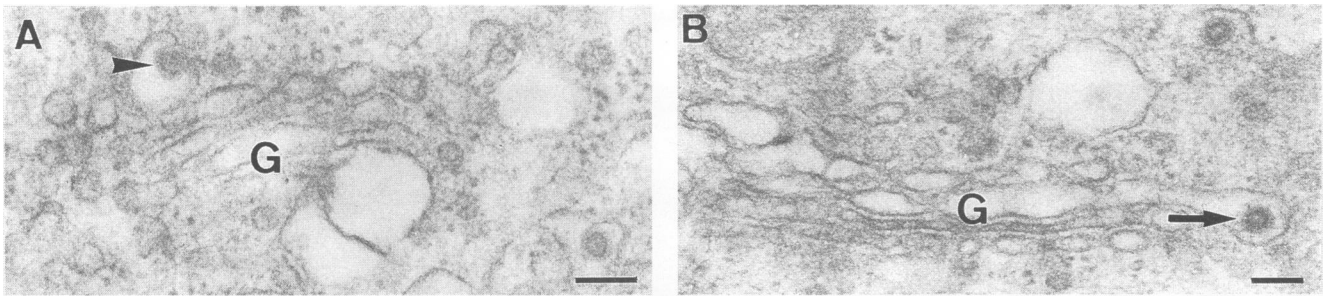


FIG. 4. CrFK cells 6 h after infection with FIPV. (A) Budding profiles (arrowhead) are restricted to pre-Golgi (G) membranes. (B) In the Golgi complex, only apparently free particles are observed (arrow). Bar, 0.1 μm.

protein had already been converted from the unglycosylated form ($M_0$) to a form which is known to be generated in the Golgi complex ($M_3$), whereas a minor fraction had even been converted to the TGR-specific $M_4$ form (22). As shown by their sensitivity to neuraminidase, both $M_3$ and $M_4$ contain sialic acid, the addition of which is considered to be a late Golgi event (20). After the 3 h of chase, virtually all vvMHV-M was converted to the $M_3$ and $M_4$ forms, indicating that by then all the M proteins had traveled at least as far as the *trans*-Golgi cisterna.

Under the same conditions, a fraction of vvIBV-M, which contains two N-linked sugar chains, acquired endo H resistance during the 3-h chase. This fraction, however, was not directly visible in the gel, probably because of the conversion to heterogeneously glycosylated forms of the polylactosaminoglycan-type oligosaccharides, which cause a diffuse migration pattern (29). The acquisition of endo H resistance is indirectly visualized by comparing the band generated after endo H digestion, representing the fraction that did not acquire complex sugars, with the band obtained after *N*-glycanase treatment, i.e., the total amount of labeled M protein. To estimate the amount of vvIBV-M acquiring endo H resistance, the

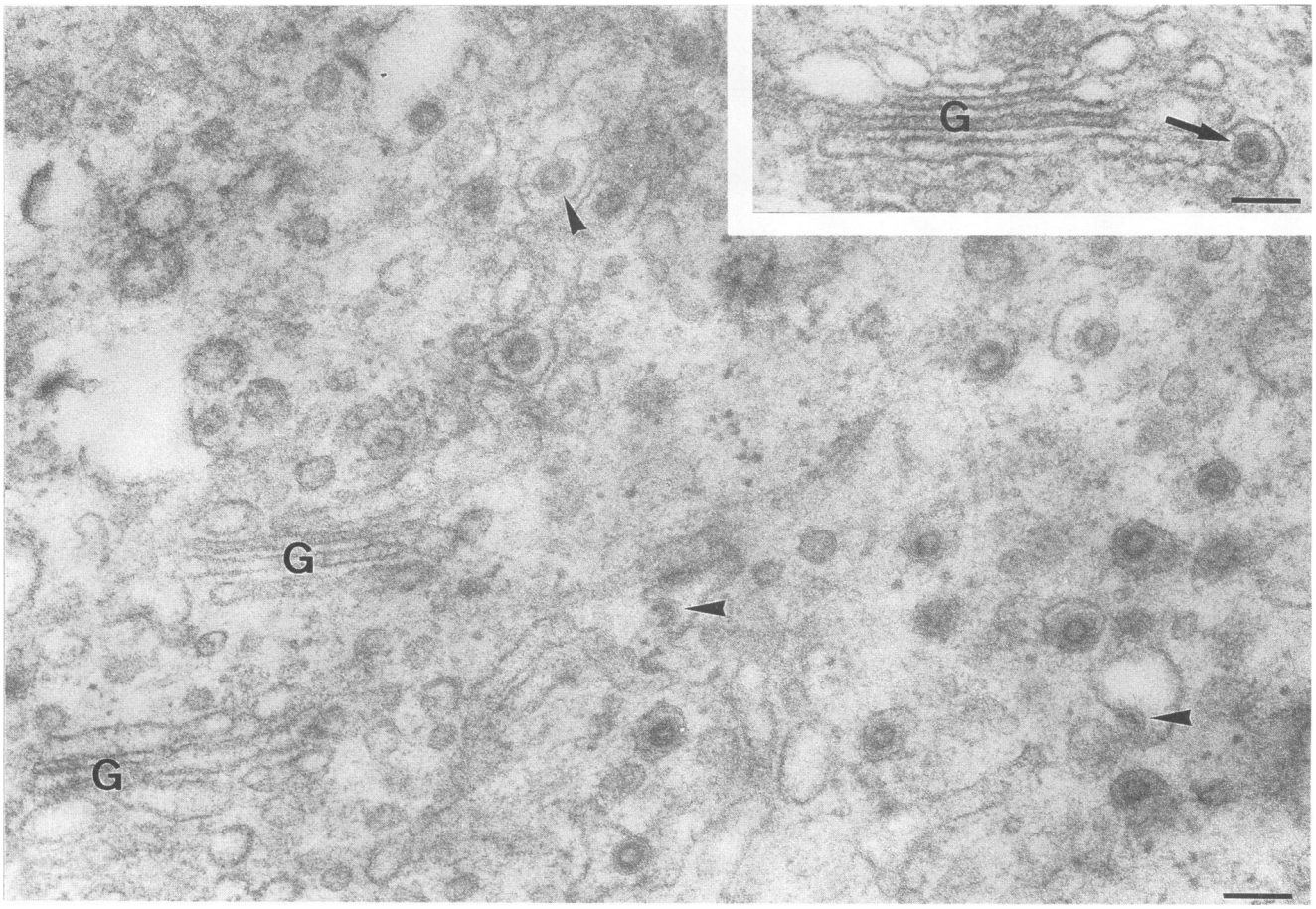


FIG. 5. Golgi (G) area of a CrFK cell 6 h after TGEV infection. Budding (arrowheads) occurs exclusively in smooth-surfaced pre-Golgi membranes. The insert shows a free TGEV particle (arrow) in the Golgi complex. Bars, 0.1 μm.

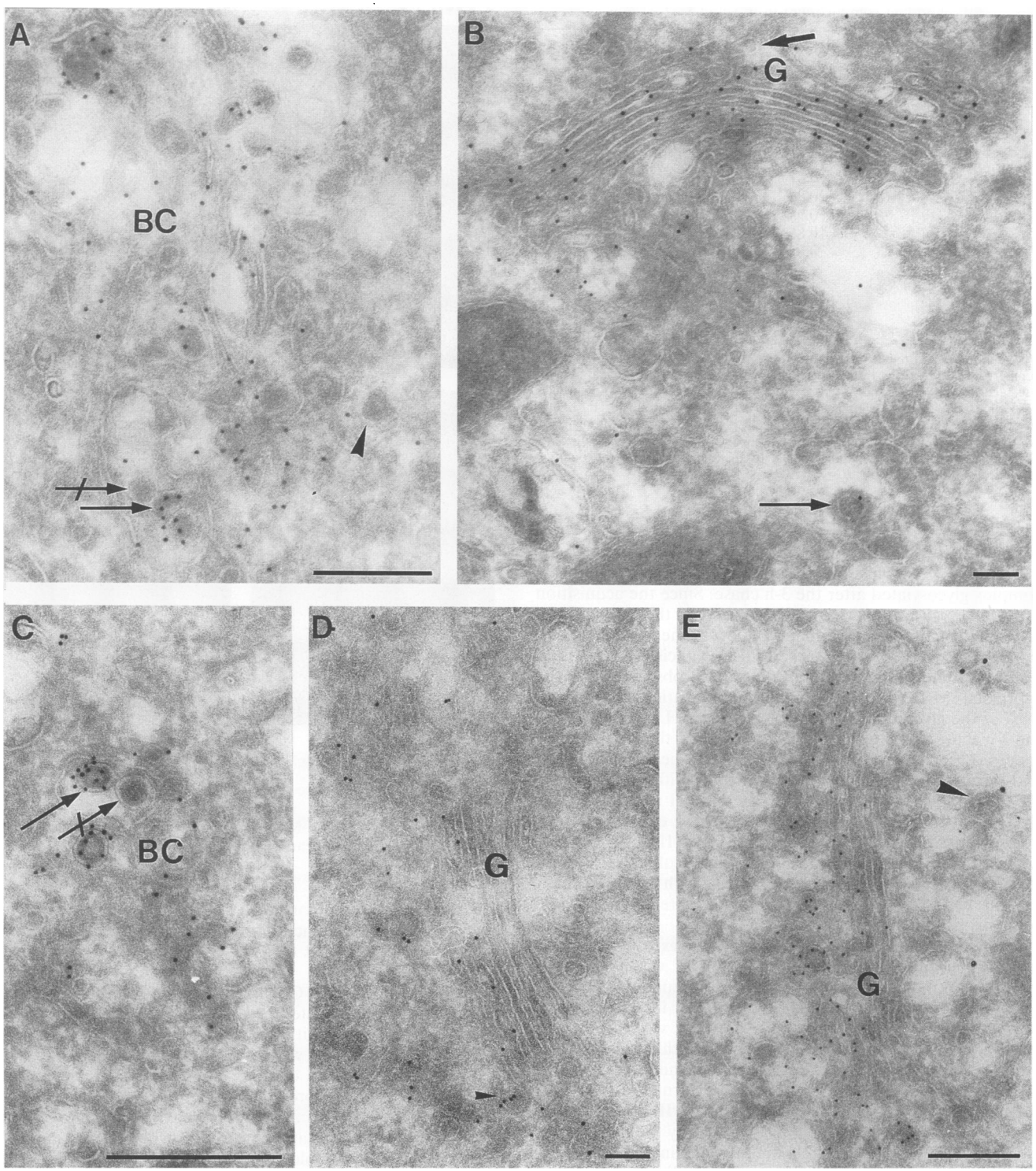


FIG. 6. Immunolabeling of MHV M (A and B) and IBV M (C to E) in infected Sac(−) cells at 6 and 8 h p.i., respectively. The budding compartment (BC) was recognized by the presence of budding profiles (arrowhead). (A) MHV M in the membranes of the budding compartment (BC) and in assembled viruses (arrow). Virions not exposing MHV M C termini are devoid of label (slashed arrow). (B) MHV M is found in all cisternae of the Golgi complex (G), although label in the *cis*-most cisterna (bold arrow) is relatively low. Little MHV M label is present in TGR membranes, some of which bear a typical clathrin coat (long arrow). (C) IBV M in membranes of the budding compartment and in assembled viruses. (D) IBV M label in the Golgi complex is restricted to the *cis*-medial cisternae. Some of the pre-Golgi membranes bear a typical nonclathrin coat (small arrowhead). (E) Double immunolabeling of IBV M (10-nm gold) and clathrin (15-nm gold). Clathrin is found only at the *trans*-Golgi, opposite the side of Golgi-associated IBV M label (large arrowhead). Bars, 0.1 μm.

TABLE 1. Density of MHV M label over Golgi membranes and the budding compartment in infected Sac(−) cells

| Cell | No. of gold particles/intersection[a] | |
|---|---|---|
| | Golgi cisternae | Budding compartment |
| 1 | 0.44 | 0.47 |
| 2 | 0.47 | 0.37 |
| | 0.31 | 0.3 |
| | 0.51 | 0.0 |
| 3 | 0.86 | 0.13 |
| 4 | 0.95 | 0.67 |
| 5 | 0.86 | 0.44 |
| 6 | 0.82 | 0.98 |
| | | 0.33 |
| 7 | 1.4 | 0.65 |
| | | 0.52 |
| Avg ± SEM | 0.74 ± 0.11 | 0.44 ± 0.08 |

[a] Quantitations were performed for MHV-infected Sac(−) cells at 6 h p.i. The number of gold particles representing MHV M was related to the number of intersections as described in Materials and Methods. A total of 288 gold particles were counted over the Golgi cisternae, and 230 were counted over the membranes of the budding compartment. In cell 2, three Golgi complexes were evaluated. The average labeling density of the Golgi membranes is significantly higher than the average labeling density of the membranes of the budding compartment (Student $t$ test; $P = 0.019$, $t = 3.18$).

bands of the autoradiogram were spectrophotometrically quantitated (53). Thus, we found that 85% of vvIBV-M was complex glycosylated after the 3-h chase. Since the acquisition of endo H resistance is considered to occur in the medial Golgi cisterna (20), this finding implies that over time, a considerable fraction of vvIBV M had reached this Golgi cisterna. Maturation to an endo H-resistant form was also observed with the expressed vvFIPV-M. In this case, quantification showed that 64% of the glycoprotein had acquired endo H resistance after the 3-h chase and thus had reached or passed the medial Golgi cisterna. Finally, vvTGEV-M was found to be transported to and through the Golgi complex. While a significant amount of the glycoprotein had already become endo H resistant during the 1-h labeling, the protein was converted completely to a heterogeneously modified form which, like vvIBV-M, could be detected only by *N*-glycanase treatment. Collectively, these experiments provide evidence that, albeit with different kinetics, all recombinant M proteins studied reach the Golgi complex.

**Subcellular distribution of independently expressed M proteins.** To establish the site of retention of vvMHV-M and vvIBV-M in more detail, we performed immunogold labeling of cryosections of HepG2 cells fixed 6 h after inoculation with recombinant vaccinia virus (Fig. 9). Both vvMHV-M and vvIBV-M were predominantly found in smooth-surfaced membranes, reminiscent of the ER-Golgi intermediate compartment (IC) (Fig. 9A and E), and in the cisternae of the Golgi complex (Fig. 9B to D). Additionally, some vvIBV-M label was found over the RER (not shown). To identify the membranes of the IC, we performed double immunolabeling of the respective M proteins and the 53-kDa protein (p53) specific for the IC and *cis*-Golgi region (45). The IC and *cis*-Golgi region were distinguished morphologically. The TGR was defined as a Golgi-associated tubulovesicular network containing CI-MPR (Fig. 9C) (8, 19). There was no specific labeling for vvMHV-M and vvIBV-M in compartments other than RER, IC, Golgi complex, and TGR.

vvMHV-M was found in all cisternae within the Golgi complex, but the labeling intensity gradually increased toward the *trans* side of the complex, where it colocalized with the *trans*-Golgi marker galactosyltransferase (Fig. 9B); little label was present in the TGR (Fig. 9C). Often vvMHV-M label was absent from the two *cis*-most cisternae. In contrast to vvMHV-M, most of the Golgi-associated vvIBV M was present within one to three cisternae at the *cis* side of the complex, where it colocalized with p53 (Fig. 9D), whereas the *trans*-Golgi region and TGR were virtually devoid of label.

These morphological data are in good agreement with our biochemical data and provide additional evidence that significant levels of MHV M and IBV M reach the Golgi complex. Moreover, they show that the distribution of MHV M and IBV M over the Golgi complex is exactly the same in the presence or absence of other viral proteins.

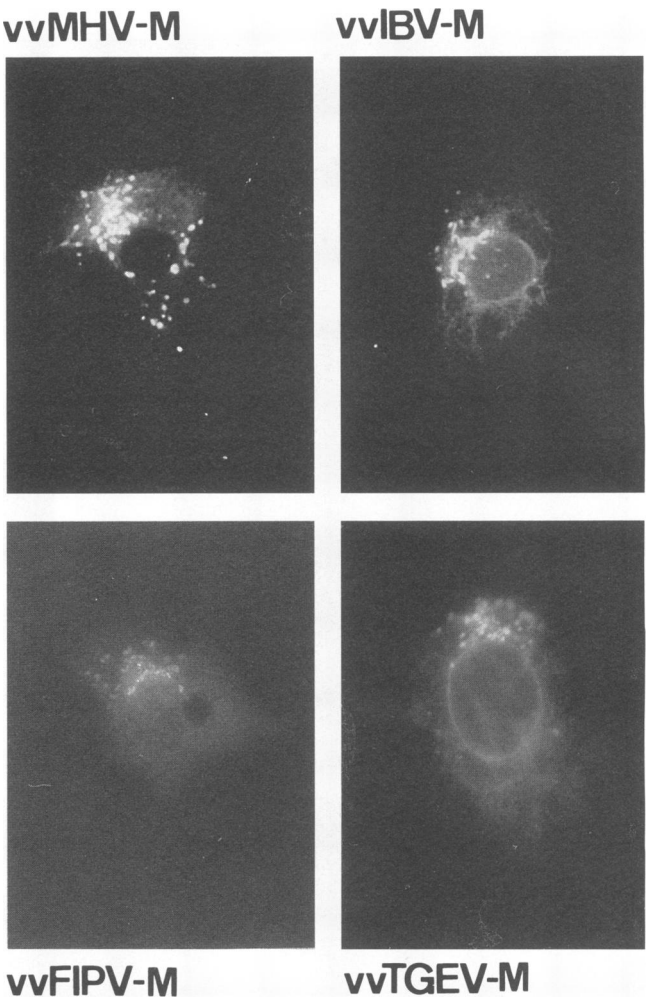


FIG. 7. Immunofluorescence staining of coronavirus M protein in HepG2 cells 6 h after inoculation with vvMHV-M, vvIBV-M, vvFIPV-M, and vvTGEV-M. All recombinant proteins accumulate intracellularly at perinuclear locations.

## DISCUSSION

We have used a combined semiquantitative immunocytochemical and biochemical approach to relate the site of accumulation of coronavirus M protein to the site of virion budding. A first prerequisite toward our goal was to establish the budding site of MHV, IBV, FIPV, and TGEV, the four

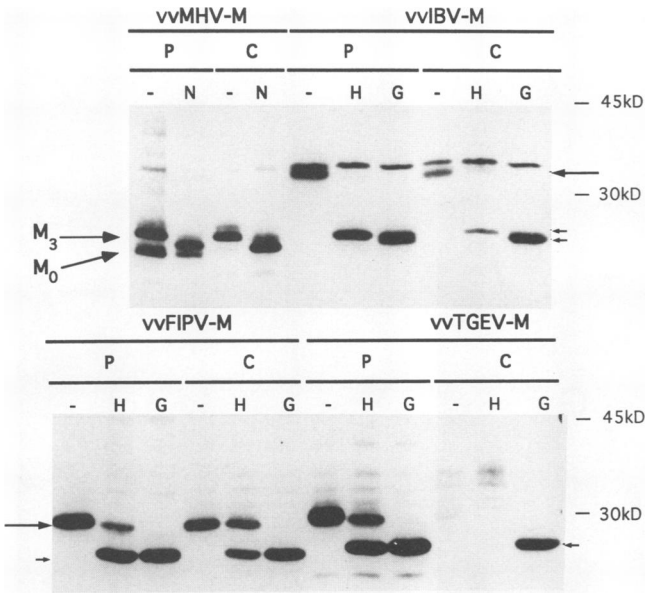


FIG. 8. HepG2 cells expressing recombinant coronavirus M proteins were metabolically labeled for 1 h (P) and chased for 3 h (C) as described in the text. Immunoprecipitated M proteins were mock treated (−) or treated with neuraminidase (N), endo H (H), or *N*-glycanase (G). The different forms of vvMHV-M are indicated. In cases of vvIBV-M, vvFIPV-M, and vvTGEV-M, the long arrows indicate the nontreated electrophoretic forms, while the short arrows indicate the faster-migrating forms obtained by endo H or *N*-glycanase treatment. Because of their heterogeneity, the forms modified by polylactosamine addition are not visible. The band migrating slightly above the untreated IBV M protein (not indicated) represents a nonglycosylated protein nonspecifically precipitated by the anti-IBV M antiserum.

coronaviruses under study. We chose a time point early in infection, when budding of MHV is restricted to smooth-surfaced membranes, which Tooze et al. (57) had termed the budding compartment. Likewise, IBV, which had been adapted to grow in Sac(−) cells, exclusively budded into the membranes of the budding compartment. Accordingly, budding profiles of FIPV and TGEV in CrFK cells were observed only in membranes morphologically similar to those of the budding compartment in Sac(−) cells. In no case was budding seen to occur in the Golgi complex. We conclude that early in infection, the four coronaviruses all bud into pre-Golgi-located membranes. Probably, coronaviruses in general initially bud into the budding compartment, as originally defined for MHV.

Next, the distribution of the various M proteins was examined by means of immunofluorescence, which showed that all accumulated in the perinuclear region and none reached the plasma membrane at detectable levels. Immunogold microscopy of MHV M and IBV M identified these perinuclear regions as the budding compartment and Golgi complex/TGR. That MHV M occurs in the Golgi cisternae of infected cells has also been observed by Tooze et al. (57) using immunoperoxidase staining. Since virus assembly did not occur at these membranes, it was inferred that at this site the protein concentration was not high enough to initiate budding. An advantage of immunogold labeling is that it allows analysis of the labeling density of a specific membrane. When we did this analysis for MHV M, the density of the label over the Golgi cisternae proved to be in the same range as or even higher than the labeling density over the budding compartment.

Subsequently we analyzed the distribution patterns of the four M proteins in the absence of other viral proteins, i.e., by expression with recombinant vaccinia viruses in HepG2 cells. Immunofluorescence staining showed that also under these conditions, the four M proteins accumulated in the perinuclear area and did not reach the plasma membrane at detectable amounts. Biochemical analysis of the oligosaccharide chains revealed that all four M proteins acquire Golgi-specific alterations (20, 22). Quantification of their different maturation forms established that within 4 h after biosynthesis, the majority had reached the Golgi (100% of MHV M and TGEV M; 85% of IBV M, and 64% of FIPV M). These observations are in agreement with our previous studies on MHV M (22) and with results reported by Machamer et al. (29). Using COS and AtT20 cells these authors immunolocalized IBV M to the *cis*-Golgi region, while some 5 to 20% of the protein had become endo H resistant during a 2-h labeling period. We subsequently located MHV M and IBV M more precisely by immunogold labeling. Both proteins were almost exclusively found in the IC and Golgi complex, with low levels of MHV M in the TGR and of IBV M in the RER. Within the Golgi complex, the two proteins showed a distribution remarkably similar to that in Sac(−) cells; MHV M was found predominantly at the *trans* side of the Golgi complex, whereas IBV M resided almost exclusively in the *cis*-to-medial cisternae, similar to what Machamer et al. (29) had observed.

Consequently, all M proteins examined must bear intrinsic retention signals which can be recognized by the host cell machinery, irrespective of the presence of other viral proteins. However, none is efficiently retained in the budding compartment. Rather, all are transported beyond the budding compartment to at least as far as the Golgi complex, some of them reaching the *trans* side and TGR. In addition, the data on MHV M and IBV M show that the distribution over the Golgi complex may be different but specific for each M protein, since in infected cells, free M proteins, i.e., proteins not incorporated in virus particles, accumulate in the same Golgi membranes as when expressed independently. Since we analyzed the distribution patterns of the two proteins in the same host cells [Sac(−) and HepG2], we can now rule out the possibility that their differential distribution is cell type specific.

Our data shed new light on the presumed role of M in coronavirus budding. Accumulation of M protein alone is not sufficient to determine the site of budding; obviously other viral and/or cellular factors are required to accomplish efficient retention of M in the budding compartment and to initiate budding. A candidate for this function is the viral spike protein (S). Supposedly, the S protein is also incorporated into virions in the budding compartment, and its interaction with the M protein might result in retention of both proteins in the budding compartment. How then can formation of spikeless virions in the presence of tunicamycin be explained (12, 41, 51)? Possibly, viral particles formed under these conditions do initially contain the S protein, which is subsequently degraded because of its incorrect conformation as a result of the absence of the N-linked oligosaccharides. This process would lead to particles containing only the residual membrane anchors and cytoplasmic tails of the S proteins. This has been demonstrated to occur in the temperature-sensitive mutant *ts*045 of vesicular stomatitis virus (4, 32).

The budding compartment ultrastructurally resembles the transitional elements at the RER as originally described for exocrine pancreatic cells (17, 58). Transitional elements have now been identified in a variety of cells and are often referred to as the ER-to-Golgi IC or salvage compartment (for reviews, see references 11, 26, and 38). It consists of a tubulovesicular

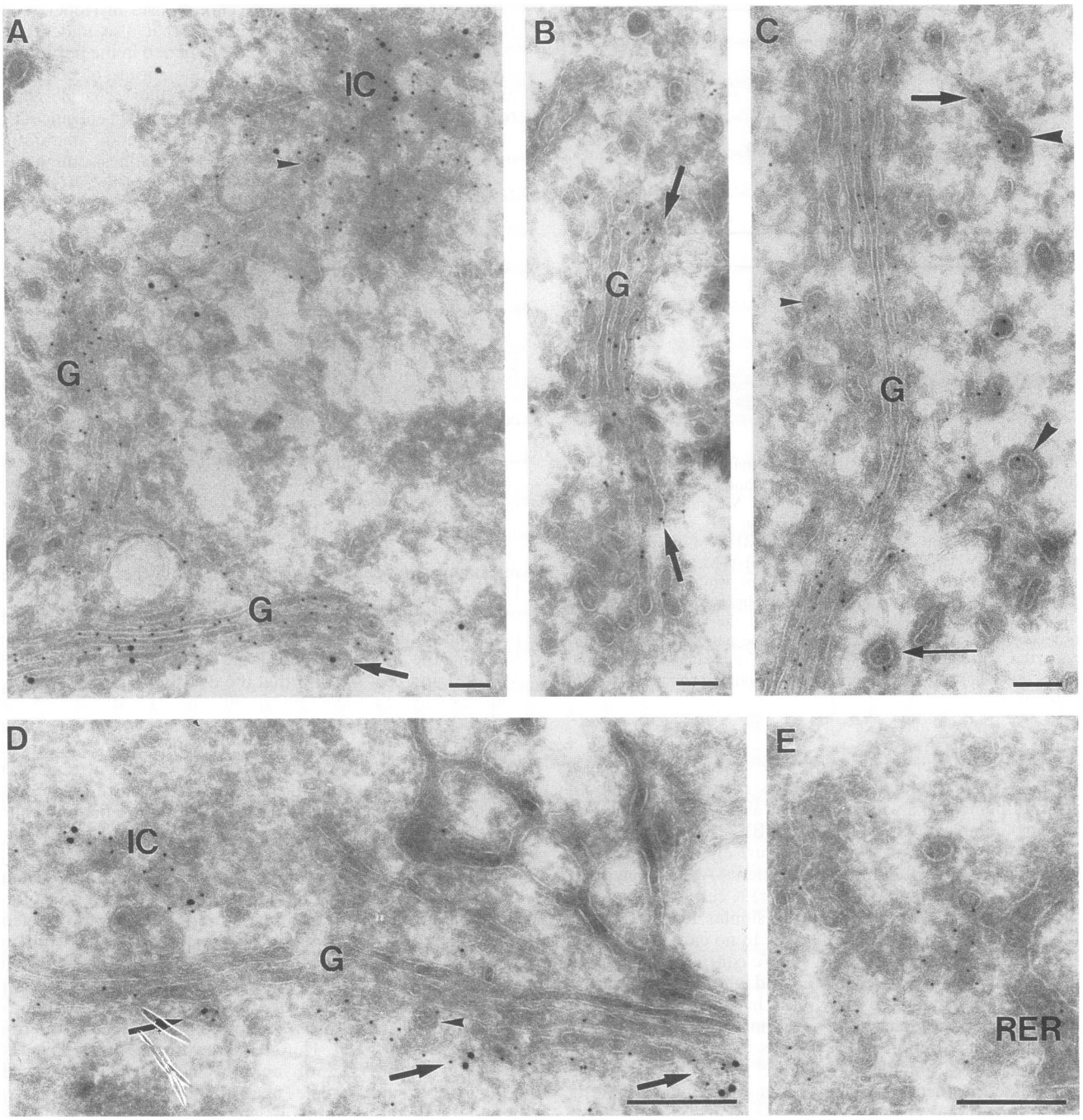


FIG. 9. Immunogold labeling of vvMHV-M (A to C) and vvIBV-M (D and E) in HepG2 cells 6 h after inoculation with vaccinia virus recombinants. (A) Double immunolabeling of vvMHV-M (10-nm gold) and p53 (15-nm gold) showing colocalization in the IC and Golgi complex (G). Note that p53 label is restricted to *cis*-Golgi elements (arrow) where vvMHV-M labeling is only low. Some of the membranes of the IC bear a typical nonclathrin coat (small arrowhead). (B) Double immunolabeling of vvMHV-M (10-nm gold) and galactosyltransferase (5-nm gold) showing colocalization in the *trans*-most cisterna (arrows) of the Golgi. (C) Double immunolabeling of vvMHV-M (5-nm gold) and CI-MPR (10-nm gold) showing a low labeling of vvMHV-M in the TGR (bold arrow). CI-MPR is often found in clathrin-coated vesicles (large arrowheads), which can be clearly distinguished from the non-clathrin-coated vesicles at the *cis* side of the Golgi complex (small arrowhead). Some vvMHV-M is also found in clathrin-coated vesicles (thin arrow). (D) Double immunolabeling of vvIBV-M (10 nm) and p53 (15 nm) showing colocalization (arrows) in the IC and in the Golgi. Note that in contrast to vvMHV-M, most of the Golgi-associated vvIBV-M is found in the *cis*-to-medial cisternae. The arrowhead indicates a non-clathrin-coated vesicle. (E) vvIBV-M in membranes of the IC that are closely apposed to an unlabeled RER cisterna.

membrane system with both perinuclear and peripheral components (44, 45) and is involved in the transport of newly synthesized proteins from the RER to the Golgi complex (27, 36, 46). In the present report, we show that independently expressed M proteins localize, in addition to the Golgi complex, only in the p53-containing IC. Moreover, we recently found that addition of GalNAc, which takes place in the MHV budding compartment (58), occurs in the IC. Together, these data led us to propose that the budding compartment is identical to the IC.

At present we can only speculate about the significance of that fraction of the M protein which is normally transported to the Golgi complex in coronavirus-infected cells. Since the proteins are not transported beyond the Golgi complex, they must be either recycled or degraded. A retrograde pathway has been proposed as a mechanism to retrieve resident proteins that have escaped from the RER (38). The site from which recycling occurs is not known, but ultrastructural and biochemical studies of a mutant cell line that retains major histocompatibility complex class I molecules in the RER have indicated that the molecules reach as far as the *cis*-Golgi region (14). Such a pathway might also serve to retrieve M proteins that have escaped the budding process. Passage of the viral membrane proteins through the Golgi complex followed by retrieval might even be a normal step in virus assembly. In that case, progeny virions in the budding compartment should contain glycoproteins bearing Golgi-specific modifications. We are presently investigating the different possibilities.

## ACKNOWLEDGMENTS

We thank A. Osterhaus (National Institute of Public Health and Environmental Protection, Bilthoven, The Netherlands) for supplying TGEV strain Purdue. Vector pSC11 was a gift from B. Moss (NIH, Bethesda, Md.). Rabbit antiserum 4735 (anti-IBV M) and vvIBV-M were generous gifts of C. Machamer (Johns Hopkins University, Baltimore, Md.). Monoclonal antibodies Cor 21 and Cor 16 (anti-FIPV M and anti-TGEV M) were kindly provided by S. Fiscus (Colorado State University, Fort Collins, Colo.). The monoclonal antibody against p53 was a kind gift of H. P. Hauri (Biocenter, Basel, Switzerland). T. van Rijn, R. Scriwanek, and M. Niekerk are acknowledged for excellent preparation of the electron micrographs.

## REFERENCES

1. **Armstrong, J., and S. Patel.** 1991. The Golgi sorting domain of coronavirus E1 protein. J. Cell Sci. **95**:191–197.
2. **Becker, W. B., K. McIntosh, J. H. Dees, and R. M. Chanock.** 1967. Morphogenesis of avian infectious bronchitis virus and a related human virus (strain 229E). J. Virol. **1**:1019–1027.
3. **Chakrabarti, S., K. Brechling, and B. Moss.** 1985. Vaccinia virus expression vector: co-expression of β-galactosidase provides visual screening of recombinant virus plaques. Mol. Cell. Biol. **5**:3403–3409.
4. **Chen, S., N. Ariel, and A. C. Huang.** 1988. Membrane anchors of vesicular stomatitis virus: characterization and incorporation into virions. J. Virol. **62**:2552–2556.
5. **David-Ferreira, J. F., and R. A. Manaker.** 1965. An electron microscope study of the development of a mouse hepatitis virus in tissue culture cells. J. Cell Biol. **24**:57–78.
6. **den Boon, J. A., E. J. Snijder, J. Krijnse Locker, M. C. Horzinek, and P. J. M. Rottier.** 1991. Another triple-spanning envelope protein among intracellularly budding RNA viruses: the Torovirus E protein. Virology **182**:655–663.
7. **Dubois-Dalcq, M. E., E. W. Doller, M. V. Haspel, and K. V. Holmes.** 1982. Cell tropism and expression of mouse hepatitis viruses (MHV) in mouse spinal cord cultures. Virology **119**:317–331.
8. **Geuze, H. J., J. W. Slot, G. J. Strous, A. Hasilik, and K. von Figura.** 1985. Possible pathways for lysosomal enzyme delivery. J. Cell Biol. **101**:2253–2262.
9. **Griffiths, G., S. Pfeiffer, K. Simons, and K. Matlin.** 1985. Exit of newly synthesized membrane proteins from the *trans*-cisterna of the Golgi complex to the plasma membrane. J. Cell Biol. **101**:949–964.
10. **Griffiths, G., and P. Rottier.** 1992. Cell biology of viruses that assemble along the biosynthetic pathway. Semin. Cell Biol. **3**:367–381.
11. **Hauri, H. P., and A. Schweizer.** 1992. The endoplasmic reticulum-Golgi intermediate compartment. Curr. Opin. Cell Biol. **4**:600–608.
12. **Hille, A., J. Klumperman, H. J. Geuze, C. Peters, F. M. Brodsky, and K. von Figura.** 1992. Lysosomal acid phosphatase is internalized via clathrin-coated pits. Eur. J. Cell Biol. **59**:106–115.
13. **Holmes, K. V., E. W. Doller, and L. S. Sturman.** 1981. Tunicamycin-resistant glycosylation of coronavirus glycoprotein: demonstration of a novel type of viral glycoprotein. Virology **115**:334–344.
14. **Hsu, V. W., L. C. Yuan, J. G. Nuchtern, J. Lippincott-Schwartz, G. J. Hammerling, and R. D. Klausner.** 1991. A recycling pathway between the endoplasmic reticulum and the Golgi apparatus for retention of unassembled MHC class I molecules. Nature (London) **352**:441–444.
15. **Jacobs, L., R. de Groot, B. A. M. van der Zeijst, M. C. Horzinek, and W. Spaan.** 1987. The nucleotide sequence of the peplomer gene of porcine transmissible gastroenteritis virus (TGEV): comparison with the sequence of the peplomer protein of feline infectious peritonitus virus (FIPV). Virus Res. **8**:363–371.
16. **Jacobse-Geels, H. E. L., and M. C. Horzinek.** 1983. Expression of feline infectious peritonitis coronavirus antigens on the surface of feline macrophage-like cells. J. Gen. Virol. **64**:1859–1866.
17. **Jamieson, J. D., and G. E. Palade.** 1967. Intracellular transport of secretory proteins in the pancreatic exocrine cell. I. Role of the peripheral elements of the Golgi complex. J. Cell Biol. **34**:577–615.
18. **Klumperman, J., J. C. Boekestijn, A. M. Mulder, J. A. M. Fransen, and L. A. Ginsel.** 1990. Intracellular localization and endocytosis of brush-border enzymes in the enterocyte-like cell line Caco-2. Eur. J. Cell Biol. **54**:76–84.
19. **Klumperman, J., A. Hille, T. Veenendaal, V. Oorschot, W. Stoorvogel, K. von Figura, and H. J. Geuze.** 1993. Differences in the endosomal distributions of the two mannose 6-phosphate receptors. J. Cell Biol. **121**:997–1010.
20. **Kornfeld, R., and S. Kornfeld.** 1985. Assembly of asparagine-linked oligosaccharides. Annu. Rev. Biochem. **54**:631–664.
21. **Krijnse-Locker, J., M. Ericsson, P. J. M. Rottier, and G. Griffiths.** 1994. Characterization of the budding compartment of mouse hepatitis virus: evidence that transport from the rough ER to the Golgi complex requires only one vesicular step. J. Cell Biol. **124**:55–70.
22. **Krijnse Locker, J., G. Griffiths, M. C. Horzinek, and P. J. M. Rottier.** 1992. O-glycosylation of the coronavirus M protein; differential localization of sialyltransferases for N- and O-linked oligosaccharides. J. Biol. Chem. **267**:14094–14101.
23. **Krijnse Locker, J., J. K. Rose, M. C. Horzinek, and P. J. M. Rottier.** 1992. Membrane assembly of the triple-spanning coronavirus M protein. J. Biol. Chem. **267**:21911–21918.
24. **Laude, H., D. Rasschaert, and J. C. Huet.** 1987. Sequence and N-terminal processing of the transmembrane protein E1 of the coronavirus transmissible gastroenteritis virus. J. Gen. Virol. **68**:1687–1693.
25. **Laviada, M. D., S. P. Videgain, L. Moreno, F. Alonso, L. Enjuanes, and J. M. Escribano.** 1990. Expression of swine transmissible gastroenteritis virus envelope antigens on the surface of infected cell: epitopes externally exposed. Virus Res. **16**:247–254.
26. **Lippincott-Schwartz, J.** 1993. Bidirectional membrane traffic between the endoplasmic reticulum and Golgi apparatus. Trends Cell Biol. **3**:81–88.
27. **Lotti, L. V., M. R. Torrisi, M. C. Pascale, and S. Bonatti.** 1992. Immunocytochemical analysis of the transfer of vesicular stomatitis virus G glycoprotein from the intermediate compartment to the Golgi complex. J. Cell Biol. **118**:43–50.
28. **Machamer, C. E., M. G. Grim, A. Esquela, S. W. Chung, M. Rolls, K. Ryan, and A. M. Swift.** 1993. Retention of a *cis*-Golgi protein requires polar residues on one face of a predicted α-helix in the transmembrane domain. Mol. Biol. Cell **4**:695–704.
29. **Machamer, C. E., S. A. Mentone, J. K. Rose, and M. G. Farquhar.**

1990. The E1 glycoprotein of an avian coronavirus is targeted to the *cis*-Golgi complex. Proc. Natl. Acad. Sci. USA **87**:6944–6948.
30. **Machamer, C. E., and J. K. Rose.** 1987. A specific transmembrane domain of a coronavirus E1 protein is required for its retention in the Golgi complex. J. Cell Biol. **105**:1205–1214.
31. **McKeirnan, A. J., J. F. Everman, A. Hargis, L. M. Miller, and R. L. Ott.** 1981. Isolation of feline coronavirus from two cats with diverse disease manifestations. Feline Pract. **11**:16–20.
32. **Metsikkö, K., and K. Simons.** 1986. The budding mechanism of spikeless vesicular stomatitis virus particles. EMBO J. **5**:1913–1920.
33. **Niemann, H., R. Geyer, H.-D. Klenk, D. Linder, S. Stirm, and M. Wirth.** 1984. The carbohydrates of mouse hepatitis virus (MHV) A59: structures of the O-glycosidically linked oligosaccharides of glycoprotein E1. EMBO J. **3**:665–670.
34. **Niemann, H., T. Mayer, and T. Tamura.** 1989. Signals for membrane-associated transport in eukaryotic cells, p. 307–365. *In* J. R. Harris (ed.), Subcellular biochemistry, vol. 19. Virally infected cells. Plenum Press, New York.
35. **Niemann, H., T. Mayer, M. Wirth, and T. Tamura.** 1987. Expression of the E1 gene of mouse hepatitis virus (MHV) *in vivo* and *in vitro*. Adv. Exp. Med. Biol. **218**:83–97.
36. **Oprins, A. R. Duduen, T. E. Kreis, H. J. Geuze, and J. W. Slot.** 1993. B-COP localizes mainly to the *cis*-Golgi side in exocrine pancreas. J. Cell Biol. **121**:49–59.
37. **Orci, L., P. Halban, M. Armherdt, O. Madsen, J.-D. Vassali, and A. Perrelet.** 1985. Clathrin-immunoreactive sites in the Golgi apparatus are concentrated at the *trans* pole in polypeptide hormone-secreting cells. Proc. Natl. Acad. Sci. USA **82**:5385–5389.
38. **Pelham, H. R. B.** 1991. Recycling of proteins between the endoplasmic reticulum and Golgi complex. Curr. Opin. Cell Biol. **3**:585–591.
39. **Petterson, R. F.** 1991. Protein localization and virus assembly at intracellular membranes. Curr. Top. Microbiol. Immunol. **179**:67–106.
40. **Pulford, D. J., and P. Britton.** 1990. Expression and cellular localisation of porcine transmissible gastroentiritis virus N and M proteins by recombinant vaccinia virus. Virus Res. **18**:203–217.
41. **Rottier, P. J. M., M. C. Horzinek, and B. A. M. van der Zeijst.** 1981. Viral protein synthesis in mouse hepatitis strain A59-infected cells: effect of tunicamycin. J. Virol. **40**:350–357.
42. **Rottier, P. J. M., and J. K. Rose.** 1987. Coronavirus E1 protein expressed from cloned cDNA localizes in the Golgi region. J. Virol. **61**:2042–2045.
43. **Sambrook, J., E. F. Fritsch, and T. Maniatis.** 1989. Molecular cloning: a laboratory manual. Cold Spring Harbor Laboratory Press, Cold Spring Harbor, N.Y.
44. **Saraste, J., G. E. Palade, and M. G. Farquhar.** 1987. Antibodies to rat pancreas Golgi subfractions: identification of a 58-kD *cis*-Golgi protein. J. Cell Biol. **105**:2021–2029.
45. **Schweizer, A., J. Fransen, T. Bächi, L. Ginsel, and H. P. Hauri.** 1988. Identification, by a monoclonal antibody, of a 53 kDa protein associated with a tubulo-vesicular compartment at the *cis*-side of the Golgi apparatus. J. Cell Biol. **107**:1643–1653.
46. **Schweizer, A., J. Fransen, K. Matter, T. E. Kreis, L. Ginsel, and H. P. Hauri.** 1990. Identification of an intermediate compartment involved in the protein transport from ER to Golgi apparatus. Eur. J. Cell Biol. **53**:185–196.
47. **Slot, J. W., H. J. Geuze, S. Gigengack, G. E. Lienhard, and D. E. James.** 1991. Immunolocalization of the insulin regulatable glucose transporter in brown adipose tissue of the rat. J. Cell Biol. **113**:123–135.
48. **Slot, J. W., H. J. Geuze, and A. J. Weerkamp.** 1988. Localization of macromolecular components by application of the immunogold technique on cryosectioned bacteria. Methods Microbiol. **20**:211–236.
49. **Spaan, W., D. Cavanagh, and M. C. Horzinek.** 1988. Coronaviruses: structure and genome expression. J. Gen. Virol. **69**:2939–2952.
50. **Spaan, W. J. M., P. J. M. Rottier, M. C. Horzinek, and B. A. M. van der Zeijst.** 1981. Isolation and identification of virus specific mRNAs in cell infected with mouse hepatitis virus (MHV-A59). Virology **108**:424–434.
51. **Stern, D. F., and B. M. Sefton.** 1982. Coronavirus proteins: structure and function of the oligosaccharides of the avian infectious bronchitis virus glycoproteins. J. Virol. **44**:794–803.
52. **Sturman, L., and K. Holmes.** 1985. The novel glycoproteins of coronaviruses. Trends Biochem. Sci. **10**:17–20.
53. **Suissa, M.** 1983. Spectrophotometric quantitation of silver grains eluted from autoradiograms. Anal. Biochem. **133**:511–514.
54. **Swift, A. M., and C. E. Machamer.** 1991. A Golgi retention signal in a membrane spanning domain of coronavirus E1 protein. J. Cell Biol. **115**:19–30.
55. **To, L. T., S. Bernard, and I. Lantier.** 1991. Fixed-cell immunoperoxidase technique for the study of surface antigens induced by the coronavirus of transmissible gastroenteritis (TGEV). Vet. Microbiol. **29**:361–368.
56. **Tooze, J., and S. Tooze.** 1985. Infection of AtT20 murine pituitary tumour cells by mouse hepatitis virus strain A59: virus budding is restricted to the Golgi region. Eur. J. Cell Biol. **37**:203–212.
57. **Tooze, J., S. Tooze, and G. Warren.** 1984. Replication of coronavirus MHV-A59 in sac(−) cells: determination of the first site of budding of progeny virions. Eur. J. Cell Biol. **33**:281–293.
58. **Tooze, S. A., J. Tooze, and G. Warren.** 1988. Site of addition of N-acetyl-galactosamine to the E1 glycoprotein of mouse hepatitis virus-A59. J. Cell Biol. **106**:1475–1487.
59. **Vennema, H., R. Rijnbrand, L. Heijnen, M. C. Horzinek, and W. J. M. Spaan.** 1991. Enhancement of the vaccinia virus/phage T7 RNA polymerase expression system using encephalomyocarditis virus 5′-untranslated region sequences. Gene **108**:201–210.
60. **Weibel, E. R.** 1979. Stereological methods I. Practical methods for biological morphometry. Academic Press Inc., New York.